

# DNA Double-stranded Breaks Induce Histone H2AX Phosphorylation on Serine 139\*

(Received for publication, July 25, 1997)

Emmy P. Rogakou, Duane R. Pilch, Ann H. Orr, Vessela S. Ivanova, and William M. Bonner‡

From the Laboratory of Molecular Pharmacology, Division of Basic Sciences, NCI, National Institutes of Health, Bethesda, Maryland 20892

When mammalian cell cultures or mice are exposed to ionizing radiation in survivable or lethal amounts, novel mass components are found in the histone H2A region of two-dimensional gels. Collectively referred to as  $\gamma$ , these components are formed *in vivo* by several procedures that introduce double-stranded breaks into DNA.  $\gamma$ -Components, which appeared to be the only major novel components detected by mass or  $^{32}\text{PO}_4$  incorporation on acetic acid-urea-Triton X-100-acetic acid-urea-cetyltrimethylammonium bromide or SDS-acetic acid-urea-cetyltrimethylammonium bromide gels after exposure of cells to ionizing radiation, are shown to be histone H2AX species that have been phosphorylated specifically at serine 139.  $\gamma$ -H2AX appears rapidly after exposure of cell cultures to ionizing radiation; half-maximal amounts are reached by 1 min and maximal amounts by 10 min. At the maximum, approximately 1% of the H2AX becomes  $\gamma$ -phosphorylated per gray of ionizing radiation, a finding that indicates that 35 DNA double-stranded breaks, the number introduced by each gray into the  $6 \times 10^9$  base pairs of a mammalian G<sub>1</sub> genome, leads to the  $\gamma$ -phosphorylation of H2AX distributed over 1% of the chromatin. Thus, about 0.03% of the chromatin appears to be involved per DNA double-stranded break. This value, which corresponds to about  $2 \times 10^6$  base pairs of DNA per double-stranded break, indicates that large amounts of chromatin are involved with each DNA double-stranded break. Thus,  $\gamma$ -H2AX formation is a rapid and sensitive cellular response to the presence of DNA double-stranded breaks, a response that may provide insight into higher order chromatin structures.

In eucaryotes, DNA is packaged into nucleosomes, which are in turn arranged in various higher order structures to form chromatin (1, 2). The nucleosome, the crystallographic structure of which has recently been elucidated (3), is composed of about 145 bp<sup>1</sup> of DNA and eight histone proteins, two from each of four histone protein families, H4, H3, H2B, and H2A. In mammals, each histone family is encoded by multiple genes, which with few exceptions are expressed in concert with replication (4). The various members of the H4, H3, and H2B fam-

ilies differ in few if any amino acid residues (5).<sup>2</sup> In contrast, the H2A family includes three subfamilies whose members contain characteristic sequence elements that have been conserved independently throughout eucaryotic evolution (6, 7). The three H2A subfamilies are the H2A1-H2A2, the H2AZ, and the H2AX; in mammals the H2AZ represents about 10% of the H2A complement, the H2AX represents 2–25%, and the H2A1-H2A2 represents the balance.

In addition, histone species are often modified with phosphate and acetate moieties on specific serine and lysine residues, respectively, usually near the amino or carboxyl termini. A specific role for histone acetylation has been confirmed with the finding that histone acetylases are transcription factors (8). Consistent with this is the finding that H4 is acetylated to higher levels in euchromatin than in heterochromatin (9). Several histone modifications are correlated with chromosome condensation and mitosis; histone H3 becomes phosphorylated on residue serine 10 (10), and linker histone H1 becomes multiply phosphorylated (11).

In this report, we demonstrate that H2AX becomes phosphorylated on residue serine 139 in cells when double-stranded breaks are introduced into the DNA by ionizing radiation. One of the three H2A subfamilies that has been conserved throughout evolution (12), H2AX comprises 2–10% of the H2A complement in mammalian tissues and larger fractions in lower eucaryotes where in budding yeast H2AX constitutes virtually all of the H2A (5). Our finding of a human astrocytoma cell line SF268 in which H2AX is 25% of the H2A complement shows that H2AX can be more than 10% of H2A complement in tissue culture cells. The sequence that differentiates the H2AX from the other two H2A subfamilies is the C-terminal motif SQ(D/E)(I/L/Y)-(end). In mammals, the serine in this motif is residue 139, the site of  $\gamma$ -phosphorylation. This report is the first demonstration of a unique *in vivo* function for H2AX, a function that clearly differentiates it from the other H2A species.

We report that exposure of cell cultures and mice to survivable as well as lethal amounts of ionizing radiation leads to the induction of  $\gamma$ -H2AX. Ionizing radiation has been present during the evolution of living systems; current background levels, about 0.5 millisieverts/year, induce on the order of  $10^5$  DNA double-stranded breaks each second in the cells of a 50-kg mammal. In tissue culture, of every 40 DNA double-stranded breaks introduced per cell by ionizing radiation, approximately one major karyotypic defect is found (13), defects that may reflect an unbalanced genome and altered cellular metabolism, perhaps leading to cell death or neoplastic progression.

We demonstrate that  $\gamma$ -H2AX formation is both a rapid and sensitive response to ionizing radiation. Half-maximal amounts of  $\gamma$ -H2AX are reached by 1 min postirradiation, and

\* The costs of publication of this article were defrayed in part by the payment of page charges. This article must therefore be hereby marked "advertisement" in accordance with 18 U.S.C. Section 1734 solely to indicate this fact.

‡ To whom correspondence and reprint requests should be addressed: NIH-NCI, Bldg. 37, Rm. 5D17, Bethesda, MD 20892. Tel.: 301-496-5942; Fax: 301-402-0752; E-mail: wmbonner@helix.nih.gov.

<sup>1</sup> The abbreviations used are: bp, base pair(s); Gy, gray; CHO, Chinese hamster ovary; TEMED, *N,N,N',N'*-tetramethylethylenediamine; BrdUrd, bromodeoxyuridine; AUT, acetic acid-urea-Triton X-100; AUC, acetic acid-urea-cetyltrimethylammonium bromide; DNA-PK, DNA-protein kinase.

<sup>2</sup> The HHGRI/NCBI Histone Sequence Database is available on the World Wide Web at <http://www.ncbi.nlm.nih.gov/Baxevani/HISTONES>.

maximal amounts are reached by 10 min. At the maximum, approximately 1% of the H2AX becomes  $\gamma$ -phosphorylated per Gy of ionizing radiation. This value, which corresponds to about  $2 \times 10^6$  bp of DNA/double-stranded break, indicates that substantial amounts of chromatin may be involved with each DNA double-stranded break. Thus,  $\gamma$ -H2AX formation is a rapid and sensitive cellular response to the presence of DNA double-stranded breaks, a response that may provide insight into higher order chromatin structures.

#### EXPERIMENTAL PROCEDURES

**Isolation and Labeling of Nuclei**—The cell cultures used in this study were grown in 10-cm dishes with RPMI 1640 medium containing 10% fetal calf serum. Nuclei from approximately  $10^7$  cells were isolated essentially as described by Whitlock *et al.* (14). Cell monolayers were washed with cold phosphate-buffered saline. One ml of lysis buffer (10 mM Tris-HCl, pH 8, 5 mM MgCl<sub>2</sub>, 0.5% Nonidet P-40) was added to each of the cell layers, which were scraped into microcentrifuge tubes, and the nuclei were pelleted for 2 s in a microcentrifuge. The histones were extracted from the pellets with 3 volumes of 0.5 M HCl for 30 min on ice and prepared for two-dimensional gel analysis.

For labeling studies, nuclear pellets were resuspended in 1 volume of TMCD assay buffer (10 mM Tris-HCl, pH 8, 5 mM MgCl<sub>2</sub>, 5 mM CaCl<sub>2</sub>, 5 mM dithiothreitol). One  $\mu$ l of [ $\gamma$ -<sup>32</sup>P]<sub>4</sub>ATP was added to 9  $\mu$ l of each of the nuclear suspensions, and the mixtures were incubated at 20 °C for 20 min. Then 100  $\mu$ l of ice-cold assay buffer was added to each of the reaction mixtures, which were spun at 1000 rpm in a microcentrifuge for 5 min; the histones were extracted from the pellets with 3 volumes of 0.5 M HCl for 30 min on ice and prepared for two-dimensional gel analysis.

**Exposure of Cell Cultures to Ionizing Radiation**—The medium of CHO, SF268 or other cell cultures was replaced with 10 ml of ice-cold medium, and the cultures were exposed to a <sup>137</sup>Cs source at a rate of either 5 or 17 Gy/min in a Shepherd Mark I irradiator. The temperature of the medium remained below 8 °C during the irradiation. After irradiation, the cold medium was replaced with medium at 37 °C, and the cultures were returned to the incubator for the times indicated. The nuclei and histones were then prepared for analysis.

**Exposure of Mice to Ionizing Radiation**—DBA/2 mice, 35 days old, were irradiated with 200 Gy for 12.5 min at 17 Gy/min or with 3.6 Gy for 1.5 min at 2.4 Gy/min. The mice were euthanized in a CO<sub>2</sub> chamber at the appropriate times. The livers, about 0.75 g, wet weight, were removed, diced, and homogenized (Polytron, Brinkmann Instruments) in 5 ml of an ice-cold buffer (10 mM Tris-HCl, pH 7.5, 1 mM MgCl<sub>2</sub>) for 10 s. Nonidet P-40 was added to a final concentration of 0.5%, and the suspension was homogenized another 10 s at a slow speed to minimize foaming. The nuclei were pelleted from a 2-ml aliquot of each homogenate by a 2-s spin in a microcentrifuge. Concentrated HCl was added to the pellets to a final concentration of 0.5 M HCl; histones were extracted for analysis.

**Two-dimensional Gel Analysis of Histones**—Nuclear suspensions were pelleted for 2 s in a microcentrifuge; the pellets were resuspended in 0.5 M HCl and extracted for 30 min on ice. Reaction mixtures containing unbound histone were made 0.5 M in HCl and extracted as above. Acid-insoluble material was pelleted for 5 min in the microcentrifuge, and the supernatants were removed to other tubes. Powdered urea was added to each of the supernatants to 8 M, phenolphthalein was added to 0.002%, and concentrated ammonia was added until the solutions became pink. Acetic acid was then added to 1 M, and the samples were loaded onto polyacrylamide gels.

Histone gels comprise a first acetic acid-urea-Triton X-100 (AUT) dimension followed by a second acetic acid-urea-cetyltrimethylammonium bromide (AUC) dimension (15). AUT gels were prepared in shells 36 cm wide, 45 cm high, and 0.4 mm thick. The resolving gel solution contained urea (8 M), acrylamide (12%), bisacrylamide (0.11%), acetic acid (1 M), ammonia (0.03 M), Triton X-100 (0.5%), TEMED (0.5%), and riboflavin (0.0004%). The solution was degassed, poured into the shells (leaving 4 cm at the top), overlaid with water-saturated butanol, and polymerized between two fluorescent light boxes for 30 min. The stacking gel solution contained urea (8 M), acrylamide (5%), bisacrylamide (0.16%), acetic acid (1 M), ammonia (0.03 M), TEMED (0.5%), and riboflavin (0.0004%). When the resolving gels had polymerized, the butanol was removed. The stacking gel solution was degassed and poured into the shells to the top. Sample combs with wells 9 mm wide and 20 mm deep were inserted into the shells, and the gels were polymerized between two fluorescent light boxes for 30 min. The reservoir buffer contained acetic acid (1 M), and glycine (0.1 M). After the

samples were loaded, electrophoresis was performed at 10 watts overnight. Finished gels were stained in a solution containing acetic acid (5%), ethanol (40%), and Coomassie Brilliant Blue R-250 (0.4%) for 30 min and destained for 30 min in a solution containing acetic acid (5%) and ethanol (20%).

AUC gels were prepared in shells 36 cm wide, 25 cm high, and 1 mm thick. The resolving gel solution contained urea (5 M), acrylamide (18.5%), bisacrylamide (0.11%), acetic acid (1 M), ammonia (0.03 M), TEMED (0.5%), and riboflavin (0.0004%). The solution was degassed, poured into the shells (leaving 4 cm at the top), overlaid with water-saturated butanol, and polymerized between two fluorescent light boxes for 30 min. The stacking gel solution contained urea (5 M), acrylamide (5%), bisacrylamide (0.16%), acetic acid (1 M), ammonia (0.03 M), TEMED (0.5%), and riboflavin (0.0004%). When the resolving gels had polymerized, the butanol was removed. The stacking gel solution was degassed, poured into the shells (leaving 2 cm at the top), and polymerized between two fluorescent light boxes for 30 min.

Regions of interest were excised from the stained first dimension gels and incubated in a solution containing acetic acid (1 M), ammonia (0.03 M), and mercaptoethylamine (1%) for 30 min. The pieces were slid into the top of a second dimension gel until they rested on the stacking gel. A solution containing 1% melted agarose, acetic acid (1 M), and ammonia (0.03 M) was poured around and to the top of the inserted sample gel; the agarose was allowed to solidify. The reservoir buffer contained acetic acid (1 M), glycine (0.1 M), and CTAB (0.15%; Sigma H-9151; hexadecyltrimethylammonium bromide). Electrophoresis was started at 67 milliamps/gel. This was about 12 watts/gel; when the wattage reached 26 watts/gel, the setting was switched to constant wattage at 26 watts until the Coomassie Blue migrated to the bottom of the gel. The total time of electrophoresis was about 7 h. Finished gels were stained in a solution containing acetic acid (5%), ethanol (40%), and Coomassie Brilliant Blue R-250 (0.4%) for 2 h and destained in a solution containing acetic acid (5%) and ethanol (20%). These gel recipes were used for all of the AUT-AUC gels presented in this paper except those shown in Fig. 1, which contained 18.5% acrylamide in the first AUT dimension; this higher concentration permitted the separation of all of the histone species but with some loss of resolution in the H2A region (Fig. 1A versus Fig. 4A). The Coomassie Blue-stained gels were recorded as TIFF images with the Eagleeye II (Stratagene Cloning Systems), the relevant images were assembled with Paint Shop Pro (Jasc, Inc) and Powerpoint (Microsoft), and the figures were printed with an HP OfficeJet Pro 1150C printer (Hewlett Packard).

**Preparation of Recombinant H2AX**—PCR was performed on plasmids containing the coding sequences for human H2A1, H2AZ, and H2AX (12), maintaining the ATG codon at the 5'-end of the coding sequence, adding a *Hind*III site just upstream of the ATG codon and a convenient restriction site at the 3'-end so that the PCR fragments could be cloned in phase into the *Hind*III site of the pET17xb vector (Novagen, Inc.). This procedure permitted the histone species to be expressed as part of fusion proteins. After constructs were checked by sequencing, duplex oligonucleotides coding for the formic acid-sensitive sequence (Asp-Pro)<sub>6</sub> followed by the nickel-binding sequence His<sub>6</sub> were inserted in phase at the *Hind*III site. The constructs were expressed in bacterial strain BL21(DE3)pLysS (Novagen, Inc.). When expression was maximal, the bacteria were harvested; the pellets were dissolved in 3 volumes of 98% formic acid and incubated at 37 °C overnight, leading to cleavage of the fusion protein species in the (Asp-Pro)<sub>6</sub> region. The formic acid was neutralized with ammonia; the solutions were dialyzed versus 10 mM Tris-HCl, pH 7.6, overnight and passed over a nickel column in the appropriate buffer (Novagen, Inc.). The histone species with their His<sub>6</sub> tags were eluted with an imidazole gradient. The eluted material was treated with CNOBr to cleave the tagged histone species at the methionine residue of the initiation codon, lyophilized, dissolved in the appropriate buffer, and passed through a nickel column to remove the His<sub>6</sub>-containing oligopeptides. The histone species were collected in the flow-through and stored at -20 °C. The recombinant histone species can be reconstituted *in vitro* into nucleosomes.<sup>3</sup> Histone H2AX mutant constructs were prepared by inserting appropriate duplex oligonucleotides at a *Sfi*I site, unique in the H2AX-pET17xb expression vector and situated in the codon for residue threonine 136.

**Nuclear Extract Labeling of Recombinant H2AX**—HeLa nuclear extracts were prepared from resuspended nuclear pellets by adding 0.1 volume of 5 M NaCl to the latter. The residual nuclei were pelleted, and the kinase extracts were used immediately. Reaction mixes (10  $\mu$ l) contained 1  $\mu$ l of 10  $\times$  TMCD assay buffer; 1  $\mu$ g of recombinant H2A1,

<sup>3</sup> V. S. Ivanova and W. M. Bonner, unpublished observations.

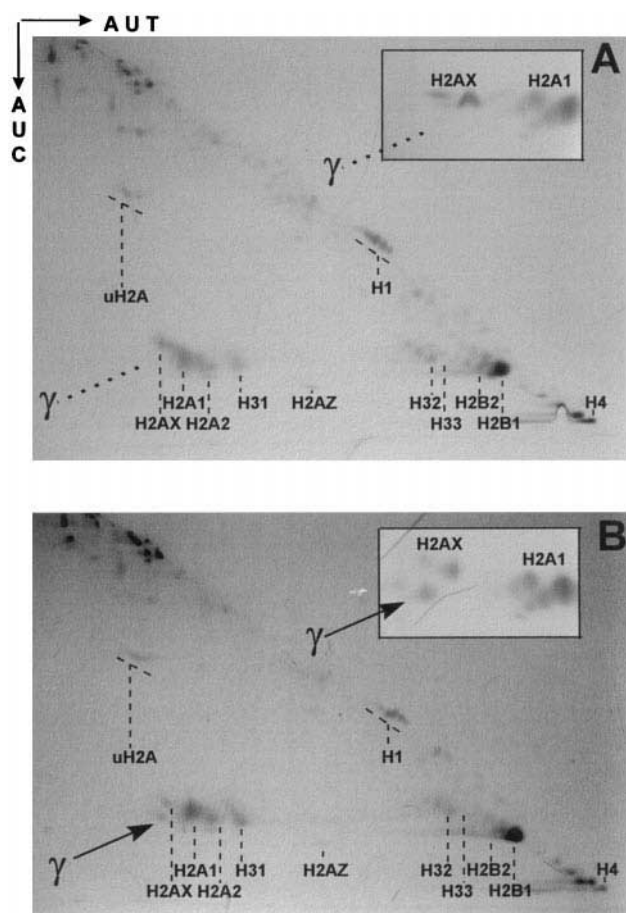


**FIG. 1. Formation of novel components in cells after ionizing radiation.** SF268 cell cultures were exposed to 50 Gy from a  $^{137}\text{Cs}$  source at the rate of 17 Gy/min and returned to the 37 °C incubator for 30 min. Histones were extracted and analyzed as described under "Experimental Procedures." The panels present gels containing 18.5% acrylamide in the AUT first dimension, while the insets present the H2A portion of gels containing 12% acrylamide in the AUT first dimension. A, control. B, gel exposed to 50 Gy. Histone species are noted; *uH2A* refers to ubiquitinated H2A species. The main novel component is noted as  $\gamma$ .

H2AX, or mutant H2AX construct; 1  $\mu\text{l}$  of [ $\gamma$ - $^{32}\text{P}$ ] $\text{ATP}$ ; and 1  $\mu\text{l}$  of nuclear kinase extract in the appropriate assay buffer. After incubation for 20 min at 20 °C, the reactions were terminated, and the histone proteins were analyzed either by two-dimensional AUT-AUC or by one-dimensional SDS gel electrophoresis.

## RESULTS

**Ionizing Radiation Induces Novel Protein Components Resolvable on Histone Gels**—When mammalian cell cultures are exposed to ionizing radiation and the acid-soluble nuclear proteins are analyzed on two-dimensional AUT-AUC gels, novel components that will be referred to as  $\gamma$  (Fig. 1, A and B) are found in the H2A region of these gels. In the first AUT dimension, histones separate according to peptide length, charge, and the ability to partition onto Triton X-100 micelles. The ability to bind Triton X-100 micelles is a property of all the known core histone species. Sensitive to single amino acid differences (16), this property enables closely related histone species to be resolved. Since the micelles are uncharged, protein molecules partitioning onto Triton X-100 micelles are retarded; this partitioning and hence the retardation can be modulated by the concentration of urea in the gel. In the second AUC dimension, the histones separate according to peptide length, charge, and shape. This combination of separation parameters resolves the histones from all other proteins on these two-dimensional gels.

In addition to permitting the resolution of closely related

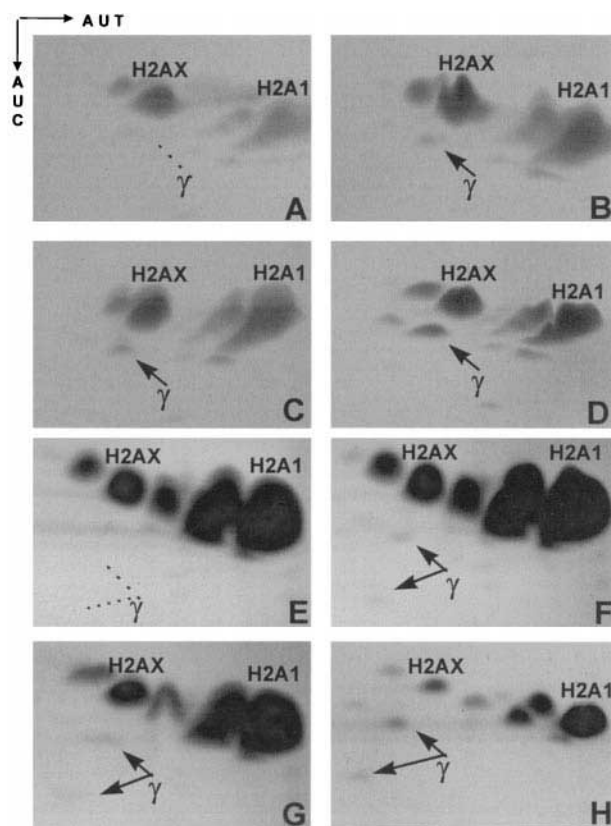


**FIG. 2. Induction of  $\gamma$ -components in cells and mice by nonlethal amounts of ionizing radiation.** A–D, SF268 cell cultures were irradiated with 0 (A), 1.2 (B), 3.6 (C), or 10.8 (D) Gy of ionizing radiation and permitted to recover for 30 min. Histones were extracted and analyzed as described under "Experimental Results." E–H, mice were irradiated, and their liver histones were prepared and analyzed as described under "Experimental Procedures." E, unirradiated mouse. F, mouse irradiated with 3.6 Gy over 1.5 min and sacrificed 15 min afterward. G, mouse irradiated with 3.6 Gy over 1.5 min and sacrificed 40 min afterward. H, mouse irradiated with 200 Gy over 12 min and sacrificed 18 min later. The position of the main novel component is noted as  $\gamma$  with an arrow when it is present and with a dotted line when it is absent or present in very low amount. In the case of mouse liver, a second arrow denotes a another  $\gamma$ -component that migrates faster in the second dimension.

histone gene products, these gels also permit the separation of post-translationally modified forms of the histone species (15). These species, which differ by single charges from each other, generally migrate just behind the parent species in both dimensions, thus forming a diagonal line (most apparent for H4 in Fig. 1, A and B). The charge differences arise most often from the phosphorylation of serine residues, which adds one negative charge to the protein and from the acetylation of lysine residues, which removes one positive charge from the protein (17). H2A (18) and to a lesser extent H2B (19) also have ubiquitin adducts; because of the size of ubiquitin, these adducts migrate in a separate region of the gel (Fig. 1, A and B).

**$\gamma$ -Components Are Formed in Cell Cultures and Mice under Nonlethal Conditions**—AUT-AUC gel analysis has been performed on other mammalian cell lines after  $^{137}\text{Cs}$  irradiation, including normal human fibroblast IMR90, transformed human fibroblast VA13, hamster CHO, human HeLa, and human HL60; all yielded similar results. Thus,  $\gamma$ -components are induced by ionizing radiation in a wide variety of mammalian cells.

To help elucidate the physiological relevance of  $\gamma$ -components, we examined whether or not they are inducible under survivable conditions. SF268 cultures were exposed to 1.2, 3.6, or 10.8 Gy of ionizing radiation and permitted to recover for 30 min.  $\gamma$ -Components were apparent in all three cases (Fig. 2,

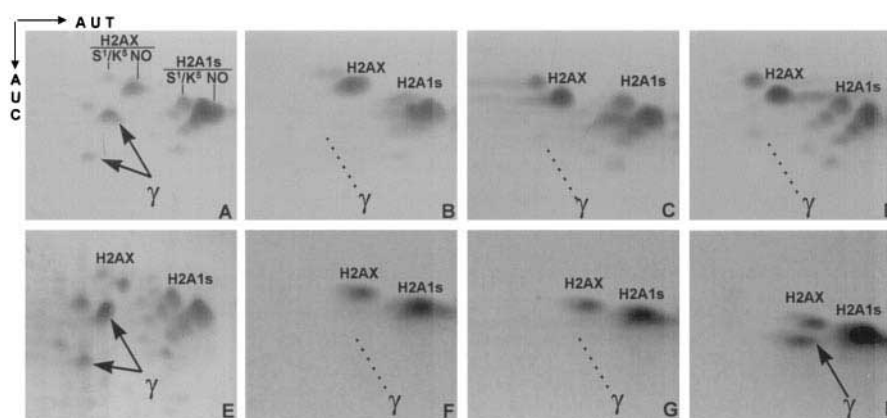


**FIG. 3. Formation of  $\gamma$ -components by other procedures that cause DNA double-stranded breaks.** A–D, SF268 cells subjected to the BrdUrd-dye-ultraviolet A light procedure. SF268 cells were grown in the presence of 0.3  $\mu$ M BrdUrd and 2.5  $\mu$ M thymidine for 44 h. The medium was removed, and the cell layers were covered with 3 ml of Hoechst dye 33258 dissolved in phosphate-buffered saline (10  $\mu$ g/ml) at 37 °C for 10 min. The dye was removed, and the cell layers were placed on ice and covered with 1 ml of ice-cold phosphate-buffered saline. The cells were exposed on ice to 10 kJ/m<sup>2</sup> ultraviolet A light from F40T12/BLB bulbs (Sylvania, 365 nm maximum), which required 16.7 min. The cold phosphate-buffered saline was removed, and warm medium was placed on the cell layers, which were returned to the 37 °C incubator for 20 min. Control cultures lacked BrdUrd, dye, or exposure to light. Histones were extracted and analyzed as described under “Experimental Procedures.” E, SF268 cells were incubated with 3 units/ml of bleomycin for 2 h. Histones were extracted and analyzed as described under “Experimental Procedures.” F–H, SF268 cultures were incubated with 10  $\mu$ M (F) or 50  $\mu$ M (G and H) H<sub>2</sub>O<sub>2</sub> for 30 min at 37 °C. The H<sub>2</sub>O<sub>2</sub>-containing medium was replaced with fresh medium, and the cells were permitted to recover at 37 °C for 30 min. Histones were extracted and analyzed as described under “Experimental Procedures,” except for the positive control (H), which was then exposed to 50 Gy and allowed to recover for 20 min at 37 °C before histone extraction. The position of the main novel component is noted as  $\gamma$  with an arrow when it is present and with a dotted line when it is absent or present in a very low amount. H2AX S<sup>1</sup>/K<sup>2</sup> refers to H2AX species containing either a phosphate on serine 1 or an acetate on lysine 5. H2AX NO refers to H2AX species with no modification. H2A1s refers to the region where H2A1 isoprotein as well as post-translationally modified species migrate. In panels A and E, a second arrow denotes a another  $\gamma$ -component that migrates faster in the second dimension.

B–D). While irradiated cells are metabolically active for several days, they may not be able to reproduce. However, cloning analysis of duplicate SF268 cell cultures showed that there was at least 40% clonal survival at 1.2 Gy and 10% clonal survival at 3.6 Gy (data not shown). Thus,  $\gamma$ -components form in cell cultures under survivable conditions.

To determine whether or not the induction of  $\gamma$ -components is a response seen in whole organisms, we exposed mice to ionizing radiation and extracted the histones from their livers. Mice were exposed to 3.6 Gy, which is 60% of the 6-Gy <sup>30</sup>LD<sub>50</sub> (50% mortality 30 days after exposure) (20–22); these mice would be expected on average to have a life span shortened by only 10–15% (23).  $\gamma$ -Components were apparent 15 (Fig. 2F) and 40 min (Fig. 2G) after exposure to 3.6 Gy.  $\gamma$ -Components were more abundant when mice were exposed to 200 Gy (Fig. 2H), which kills mice within several hours. Thus,  $\gamma$ -components form in living organisms at both nonlethal and lethal amounts of ionizing radiation.

**$\gamma$ -Components Are Induced by DNA Double-stranded Breaks**—Since the formation of  $\gamma$ -components appeared to be a widespread cellular reaction to ionizing radiation among mammals, it is relevant to determine whether the cell cultures are responding directly to the ionizing radiation or to a particular type of cellular damage induced by the ionizing radiation. Ionizing radiation introduces many different kinds of damage into cells, directly by collision with atoms of biological molecules and indirectly by collision with water molecules. The latter generates free radicals, of which the most abundant is the hydroxyl radical. Ionizing radiation produces high local concentrations of hydroxyl radicals that, if located next to a DNA molecule, may produce locally multiply damaged sites (13) containing alterations of the base and sugar residues and breaks of one or both strands of the DNA double helix.

Several agents and procedures that do or do not introduce double-stranded breaks into the DNA in cells were examined (Fig. 3). Cellular DNA can be sensitized to form DNA double- and single-stranded breaks upon irradiation with ultraviolet A light (350 nm) when cell cultures are grown in the presence of

BrdUrd and incubated with Hoechst dye 33258 just before irradiation (24). Like ionizing radiation, this method introduces double-stranded breaks as well as single-stranded breaks into DNA, but unlike the former, the mechanism is nonradiolytic. The procedure was found to result in the formation of  $\gamma$ -components in SF268 cells (Fig. 3, A–D) but only if BrdUrd, dye, and light were all present. Since this procedure leads to the formation of DNA breaks by a nonradiolytic mechanism and without hydroxyl radical formation in cells,  $\gamma$ -components are not a cellular response directly to ionizing radiation or to the presence of hydroxyl radicals, but to the presence of DNA breaks. This result was substantiated by the presence of  $\gamma$ -components when SF268 cell cultures were incubated with bleomycin (25), a compound that also introduces double- and single-stranded breaks into cellular DNA by a nonradiolytic mechanism (Fig. 3E).

While the above described procedures introduce DNA double- and single-stranded breaks without hydroxyl radical formation, H<sub>2</sub>O<sub>2</sub> produces hydroxyl radicals and DNA single-stranded breaks, as does ionizing radiation, but does not produce significant amounts of DNA double-stranded breaks because the cellular distribution of the hydroxyl radicals differs between the two agents (26). With H<sub>2</sub>O<sub>2</sub>, radicals are generated homogeneously throughout the cell as contrasted to the heterogeneous distribution found with ionizing radiation. Incubation of SF268 cell cultures with 10  $\mu$ M (Fig. 3F) or 50  $\mu$ M (Fig. 3G) H<sub>2</sub>O<sub>2</sub> for 30 min did not lead to detectable formation of  $\gamma$ -components, although these cultures were still able to form  $\gamma$ -components after exposure to ionizing radiation (Fig. 3H). These concentrations are damaging to cells; incubation of CHO cultures with 50  $\mu$ M H<sub>2</sub>O<sub>2</sub> for 30 min at 37 °C was found to result in approximately 95% clonal lethality (27). Another agent that damages cellular DNA primarily by introducing single-strand lesions (26) is ultraviolet C light. When SF268 cell cultures were irradiated with 1, 3, 10, 30, or 100 J/m<sup>2</sup> of ultraviolet C radiation, amounts of radiation that cover the range from little if any cellular effect to complete lethality, no  $\gamma$ -components were detected after a 30-min recovery (data not

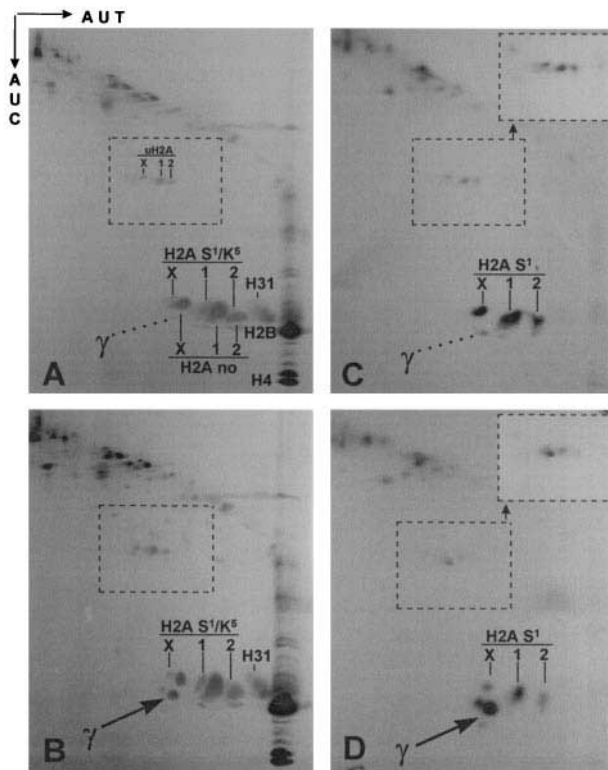


**FIG. 4. Phosphorylation of  $\gamma$ -components: AUT-AUC gels.** SF268 cells were grown almost to confluence on 10-cm dishes. *A* and *C*, one dish was incubated for 30 min at 37 °C with 5 ml of  $\text{PO}_4$ -free RPMI 1640 medium with 10% fetal calf serum and containing 1 mCi of  $^{32}\text{PO}_4$  (1000 mCi/mmol; NEN Life Science Products). *B* and *D*, a duplicate dish received 50 Gy on ice and then was incubated as above. Histones were extracted and analyzed as described under "Experimental Procedures." *A* and *B*, Coomassie Blue stain. *C* and *D*, autoradiograph. The position of the main novel component is noted as  $\gamma$  with an *arrow* when it is present and with a *dotted line* when it is absent or present in a very low amount. The *dotted boxes* outline the ubiquitinated H2A region in *panels A–D*, and in *panels C* and *D*, a longer exposure of the boxed area is reproduced in the *upper right corner*. The other nomenclature is explained in the legends to Figs. 1 and 3.

shown). Thus, it is the DNA double-stranded break from ionizing radiation that is responsible for  $\gamma$ -component formation.

**$\gamma$ -Components Are Phosphorylated H2A Derivatives**—The AUT-AUC gels shown in Fig. 1 were prepared with a 18% first dimension AUT gel to resolve all histone species. The AUT-AUC gels shown in the other figures were prepared with a 12% first dimension AUT gel to optimize the separation of  $\gamma$ -components; however, H4, H2B, and several of the H3 isoforms migrate at the buffer front in this dimension and thus are separated only in the second.  $\gamma$ -Components were obtained when SF268 cultures were exposed to 50 Gy of ionizing radiation and returned to a 37 °C incubator for a 30-min recovery period (Figs. 1*B* and 4*B*). When  $^{32}\text{PO}_4$  was included in the medium during the recovery period,  $\gamma$ -components became radioactively labeled (Fig. 4*D*). The pattern of the  $\gamma$ -components appeared to mimic the pattern of the H2AX species with its previously characterized modified forms (17). H2AX, as well as H2A1 and H2A2, can be phosphorylated on residue serine 1 and/or acetylated on residue lysine 5 (noted as H2A S<sup>1</sup>/K<sup>5</sup> on Fig. 4*A*) and/or ubiquitinated on residue lysine 119 (uH2A, inside the *dotted rectangle* in Fig. 4*A*). The phosphorylation of serine 1 accounts for the presence of  $^{32}\text{PO}_4$  label found in the H2A region in the control cultures (noted as H2A S<sup>1</sup> in Fig. 4*B*). After  $^{137}\text{Cs}$  irradiation, labeling on H2A serine 1 was decreased, while the  $\gamma$ -components became heavily labeled (Fig. 4, *C* and *D*). Note that the  $\gamma$ -components appear to be ubiquiti-

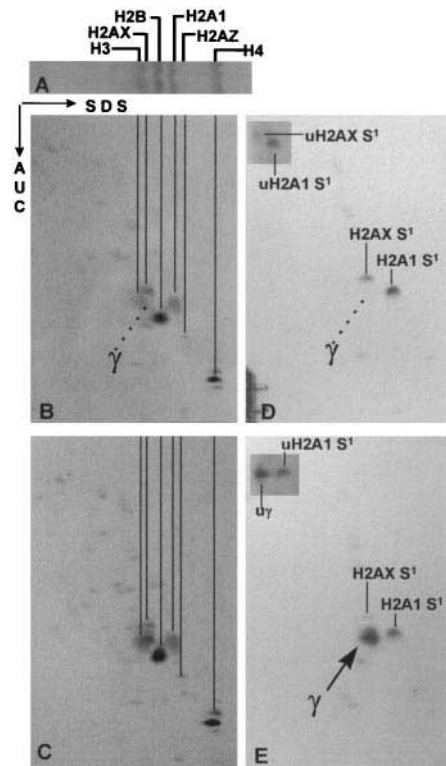


**FIG. 5. Phosphorylation of  $\gamma$ -components: SDS-AUC gels.** SF268 cells were grown almost to confluence on 10-cm dishes. *A*, first dimension SDS gel used for the two-dimensional gel presented in *panel B*. *B* and *D*, one culture was incubated for 30 min at 37 °C in 5 ml of  $\text{PO}_4$ -free RPMI 1640 medium with 10% fetal calf serum and containing 1 mCi of  $^{32}\text{PO}_4$  (1000 mCi/mmol; NEN Life Science Products). *C* and *E*, a duplicate culture received 50 Gy on ice and then was incubated as above. Histones were extracted and analyzed as described under "Experimental Procedures." *A* and *B*, Coomassie Blue stain. *C* and *D*, autoradiograph. The position of the main novel component is noted as  $\gamma$  with an *arrow* when it is present and with a *dotted line* when it is absent or present in a very low amount. The ubiquitinated H2A region shown in *panels D* and *E* is from a longer exposure. The other nomenclature is explained in the legends to Figs. 1 and 3.

nated to the same extent as the H2A species when detected by mass (inside the *dotted rectangles*, Fig. 4, *A* and *B*) and by label (inside the *dotted rectangles*, Fig. 4, *C* and *D*). These results from AUT-AUC gels indicate that the  $\gamma$ -components are phosphorylated H2A derivatives.

To obtain more information about the identity of  $\gamma$ -components, similarly prepared samples were subjected to SDS-AUC gel analysis. In SDS gels (Fig. 5*A*), proteins separate primarily according to size. H2AX migrates almost coincidentally with H3 in SDS gels, but the two are resolved on AUC gels (Fig. 5, *B* and *C*).  $\gamma$ -Components were not apparent on SDS-AUC gels by Coomassie Blue stain (Fig. 5, *B* and *C*) but were apparent when the  $^{32}\text{PO}_4$  label was detected (Fig. 5, *D* and *E*), because  $\gamma$ -components migrate coincidentally with H3 in both SDS and AUC gels, but not in AUT gels. Thus, to separate  $\gamma$ -components from other proteins it is necessary to utilize AUT gels to resolve the histone species followed by AUC gels to resolve the  $\gamma$ -components from the known modified forms of H2AX.

AUT-AUC and SDS-AUC gels contain many other proteins, only some of which are detectable by Coomassie Blue stain. Of components that were visible in these experiments either by stain or by  $^{32}\text{PO}_4$  labeling, the  $\gamma$ -components were by far the most heavily labeled and the only major ones induced by  $^{137}\text{Cs}$  irradiation (Figs. 4 and 5). It is also apparent that either with or without  $^{137}\text{Cs}$  irradiation of these cultures, there was no significant  $^{32}\text{PO}_4$  incorporation into H3 (Fig. 4, *C* and *D*) or into

the H2B and H4 species (Fig. 5, D and E).

**$\gamma$ -Components Can Be Formed *in Vitro***—We had found that  $^{32}\text{PO}_4$ -labeled  $\gamma$ -components can be generated *in vitro* with isolated nuclei and in nuclear extracts with recombinant H2AX. These findings stemmed from reports that a histone, originally identified as H3 from SDS gels (14, 28, 29) and later as H2AX (30), was the only protein labeled to a significant extent when isolated nuclei were incubated with  $[\gamma\text{-}^{32}\text{PO}_4]\text{ATP}$ . The report of H2AX as the labeled histone species (30) utilized an AUT-SDS gel system and thus did not resolve  $\gamma$ -components from H2AX, since, as shown in Figs. 4 and 5,  $\gamma$ -components and

H2AX do not resolve from each other in either of these systems. However, with the multiplicity of  $\gamma$ -components (Fig. 6B), the relationship of  $\gamma$ -components to H2AX appears even more compelling. More components are visible for two reasons. The first is the higher specific activity attainable with *in vitro* radioactive labeling. The second is the growth of the cells in 5 mM sodium butyrate for several hours before harvest, a condition that leads to increased acetylation of histone (14). Under these *in vitro* labeling conditions, mass amounts of  $\gamma$ -components are not expected, since there is no source of bulk phosphate and ATP (Fig. 6, A and B). The *in vitro* labeling of nuclei is also neither dependent on nor increased by exposure of the nuclei to ionizing radiation; this finding is possibly due to the introduction of DNA double-stranded breaks during the centrifugation steps used to isolate nuclei.

The kinase activity can be extracted with 0.35 M NaCl from nuclei and is capable of phosphorylating histones in solution (14). We prepared recombinant H2A1, H2AZ, and H2AX species and examined their ability to be phosphorylated with 0.35 M NaCl extracts. Only H2AX could be labeled with  $[\gamma\text{-}^{32}\text{PO}_4]\text{ATP}$  to a significant extent with these extracts; in addition, the labeled material migrated primarily as  $\gamma$ -components (Fig. 6, C and D).  $\gamma$ -Components did not result when recombinant H2AX was labeled with protein kinase C; the radioactive material migrated on AUT-AUC gels at the position of H2AX phosphorylated on residue serine 1 (data not shown). Thus, these *in vitro* experiments confirm that  $\gamma$ -components are H2AX derivatives.

**$\gamma$ -Component Is H2AX-phosphorylated on Serine Residue 139**—The finding that recombinant H2AX forms  $^{32}\text{PO}_4$ -labeled  $\gamma$ -components enabled us to identify the site of modification(s) as well as the recognition parameters of the relevant kinase. The strategy to localize the site of  $\gamma$ -phosphorylation utilizing recombinant H2AX is presented in Fig. 7, which displays the sequences of H2A1 and H2AX. The two sequences are almost identical up to residue lysine 119, but differ both in sequence and length in the C-terminal region. As mentioned previously, the serine at position 139 is the prime candidate for the site of  $\gamma$ -phosphorylation, since it has been conserved throughout evolution in at least one H2A species in each animal species examined.

H2AX protein has glutamic acid residues at positions 92 and 141 with no intervening aspartic acid and arginine residues. Digestion with the protease StaphV8, which cleaves at aspartic and glutamic acid residues, would be expected to yield a polypeptide 49 residues long, while clostripain digestion would be expected to generate a 57-residue C-terminal fragment that subsumes the 49-residue StaphV8 polypeptide (Fig. 7). In contrast, trypsin digestion would be expected to generate small C-terminal fragments. This C-terminal region of the H2AX

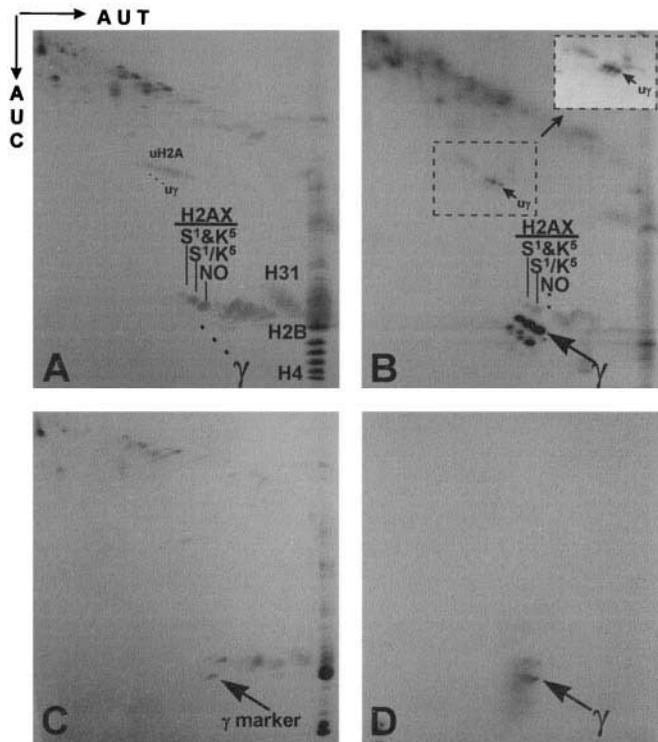
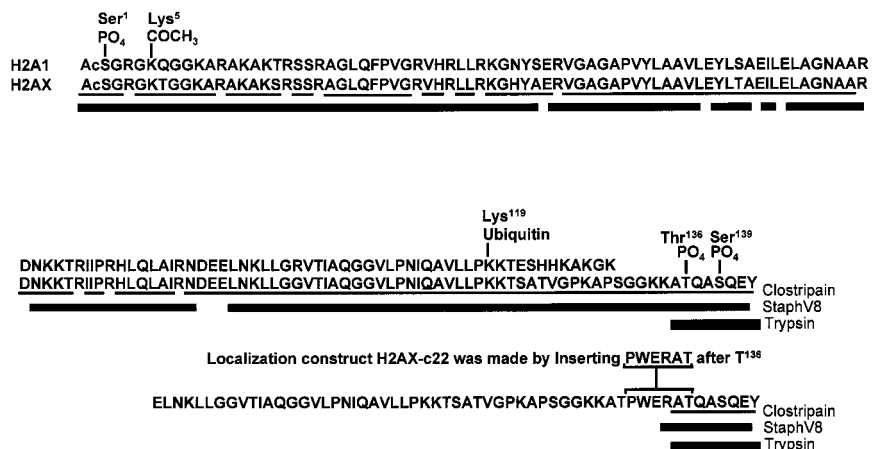


**FIG. 6.  $\gamma$ -component formation *in vitro*.** A and B, nuclei prepared from SF268 cells were incubated with  $[\gamma\text{-}^{32}\text{PO}_4]\text{ATP}$  as described under “Experimental Procedures.” The cell cultures were incubated for 3 h before nuclear isolation with 5 mM sodium butyrate to increase *in vitro* labeling (14). C and D, phosphorylation of recombinant H2AX by nuclear extract as described under “Experimental Procedures.” Carrier histone from SF268 cells irradiated with 50 Gy was added before loading the gel. A and C, Coomassie Blue stain. B and D, autoradiographs. The position of the main novel component is noted as  $\gamma$  with an arrow when it is present and with a dotted line when it is absent or present in a very low amount. H2AX S<sup>1</sup>&K<sup>5</sup> refers to H2AX species containing a phosphate on serine 1 and an acetate on lysine 5. The other nomenclature is explained in the legends to Figs. 1 and 3.

**FIG. 7. Sequences of H2A1, H2AX, and recombinant H2AX constructs.**

Light and medium lines indicate the lengths of peptides formed, respectively, by clostripain and StaphV8 cleavage of H2AX; the short heavy line indicates the H2AX C-terminal peptide derived from trypsin digestion. The identities of the five proven and putative H2AX modification sites discussed in this work are shown with the affected amino acid residue. The bacterial expression plasmid encoding human H2AX was altered by the insertion of oligonucleotides coding for ATPWER (H2AX-c22) or AAPWER (H2AX-c23) at a SfiI site of the human H2AX sequence by standard cloning techniques, and recombinant proteins were produced as described under “Experimental Procedures.”



sequence is the only region in any core histone that yields similarly sized large peptides with clostripain and StaphV8.

To confirm that  $\gamma$ -components contain phosphate in the predicted region, natural  $^{32}\text{PO}_4$ -labeled  $\gamma$ -component was digested with clostripain, StaphV8, and trypsin. Digestion with the first two resulted in large similarly sized radioactive fragments, while trypsin digestion resulted in a small one (Fig. 8A). Next, recombinant H2AX labeled with  $[\gamma\text{-}^{32}\text{PO}_4]\text{ATP}$  and nuclear kinase was digested with the same enzymes and was found to yield the same pattern of fragments (Fig. 8B, the lanes noted as 0 under none (N), trypsin (T), clostripain (C), and StaphV8 (S)) to that obtained with the natural  $\gamma$ -component. Thus,  $\gamma$ -component is a form of H2AX phosphorylated in the C-terminal region.

To determine which residue is involved in the  $\gamma$ -phosphorylation of H2AX, we prepared two recombinant H2AX derivatives with altered amino acid sequences (Fig. 7) that would provide new cleavage sites at predicted positions for the enzymes mentioned above. Clostripain digestion of the parent H2AX-c0 construct labeled with nuclear extract and  $[\gamma\text{-}^{32}\text{PO}_4]\text{ATP}$  yielded a large but less than full-length labeled peptide consistent with a

size of 57 residues (Fig. 7), while in construct H2AX-c22 (Fig. 7) almost all of the label was found in a small peptide consistent with the predicted size of 8 residues (Fig. 8B). Digestion with StaphV8 also yielded new small peptides with construct H2AX-c22 as predicted, substantiating the result with clostripain. StaphV8 digestion would also be expected to remove the terminal tyrosine, indicating that the phosphorylation takes place on the peptide ATQASQE (Fig. 8B). In construct H2AX-c23, an alanine residue replaces the threonine residue to yield a tryptic peptide AAQASQEY; that this construct is phosphorylated to a similar extent as is H2AX-c22 indicates that threonine residue 136 is not a major phosphorylation site but may be a secondary site. Histones do not contain tryptophan, thus *N*-bromosuccinimide treatment under conditions that cleave proteins only at tryptophan residues does not cleave construct H2AX-c0 (Fig. 8B, N); however, construct H2AX-c22 is cleaved under these conditions to yield a small labeled peptide consistent with the expected size (Fig. 8B, N). These results demonstrate that  $\gamma$ -components are H2AX species phosphorylated on serine 139.

**Recognition Site for  $\gamma$ -Phosphorylation**—A major advantage of using recombinant H2AX constructs to determine the site of phosphorylation is that they also allow us to determine some of the recognition parameters of the kinase for  $\gamma$ -phosphorylation. To do so, a second set of recombinant H2AX derivatives were prepared with various alterations in the C-terminal sequence (Table I). Substituting serine 139 with leucine decreased activity of the construct to 9.6% of the H2AX control, an expected finding, since this is the site of phosphorylation; however, glutamine 140 appeared to be just as essential (H2AX-c9). Neither of these constructs gave activities as low as that of H2A1, however (compare H2AX-c1 and H2AX-c9 with H2A1-wt), possibly due to a small amount of phosphorylation at threonine 136 in the H2AX constructs. Supporting this possibility is the finding that threonine did appear to substitute well for serine 139 (H2AX-c8). Glutamate 141 appeared to be relatively unimportant to the specificity (H2AX-c7). Changes in length that placed serine 139 either closer to or farther from the C terminus appeared to be of lesser importance (H2AX-c2, -c3, and -c6). On the other hand, that there may be other determinants of specificity was indicated by the low activity of constructs H2AX-c4 and c5, in which the SQ motif was present but in different backgrounds. These results show that the SQ sequence is an important determinant for  $\gamma$ -phosphorylation of H2AX.

These findings allow us to assign structures to each of the modified H2AX species. Fig. 9A presents an enlargement of the H2AX and  $\gamma$ -component region from the gel presented in Fig. 6B. A grid is superimposed over the pattern of H2AX and

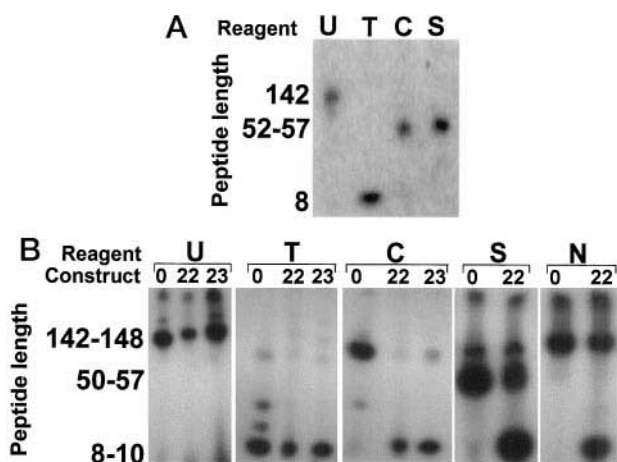


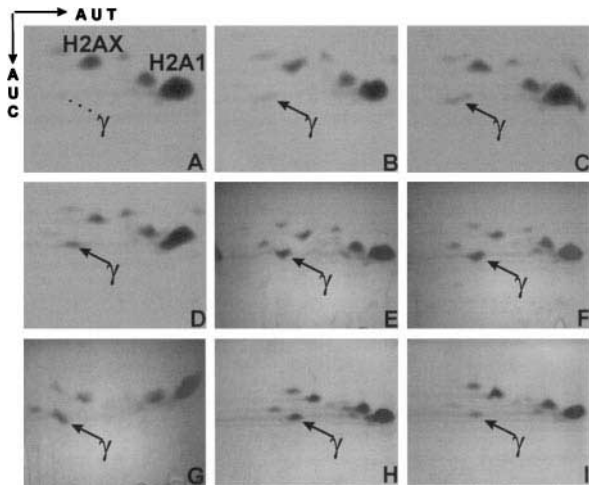
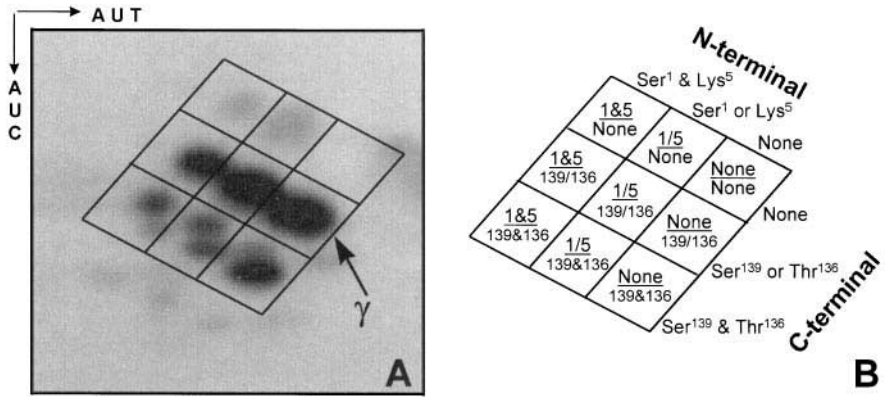
FIG. 8. **Peptides of  $\gamma$ -H2AX.** A, natural  $\gamma$ -component labeled with  $[\gamma\text{-}^{32}\text{PO}_4]\text{ATP}$  in whole nuclei was isolated from the gel, electroeluted, dialyzed against water, and freeze-dried. The material was dissolved in the appropriate buffers and incubated with water (U), trypsin (T), clostripain (C), or staphylococcus V8 (S) (all from Promega). B, recombinant protein constructs H2AX-wt, -c22, and -c23 were labeled as described under "Experimental Procedures" and incubated as above and with *N*-bromosuccinimide (Sigma). All digests were mixed with one volume of  $2 \times$  SDS sample buffer, boiled for 5 min, and analyzed by electrophoresis on 30% acrylamide gels containing SDS. The wet gels were immediately exposed to film at room temperature.

TABLE I  
Activity of altered H2AX analogues as nuclear kinase substrates

Constructs were prepared and assayed as described under "Experimental Procedures." SDS gels were stained with Coomassie Blue, and the radioactivity was assayed with the Betagen.

Construct	Sequence	Alteration	Percentage of wild type
<b>Controls</b>			
H2AX-wt	(133 residues)-katqasqey-COOH	H2AX control	100
H2A1-wt	(132 residues)	H2A1 control	2.2
<b>Single residue substitutions</b>			
H2AX-c1	(133 residues)-katqaLqey-COOH	Ser-139 to Leu	9.6
H2AX-c8	(133 residues)-katqaTqey-COOH	Ser-139 to Thr	52.0
H2AX-c9	(133 residues)-katqasNey-COOH	Gln-140 to Asn	7.2
H2AX-c7	(133 residues)-katqasqNy-COOH	Glu-141 to Asn	49.0
<b>Changes in length</b>			
H2AX-c3	(133 residues)-katqasqeyGK-COOH	Add GK to C terminus	76.0
H2AX-c6	(133 residues)-katqasq-COOH	Delete C-terminal Tyr	42.0
H2AX-c2	(133 residues)-katqasq-COOH	Delete C-terminal EY	22.0
<b>Multiresidue changes</b>			
H2AX-c5	(21 residues)-katqasqey-COOH	Delete N-terminal 112 residues	2.9
H2AX-c4	(133 residues)-katqalhhksqtk-COOH	Rat testes C-terminal hybrid	4.6

**FIG. 9. Assignment of  $\gamma$ -H2AX derivatives to particular structures.** A, an enlargement of the *in vitro* labeled material presented in Fig. 6B with a grid superimposed. B, the same grid with the modified forms present in each square. 1/5 refers to H2AX species modified in the 1- or the 5-position, as presented in Fig. 7. 1&5 refers to H2AX species modified in both positions. Modifications at positions 136 and 139 are likewise noted.



**FIG. 10. Relative amount of  $\gamma$ -H2AX at various times after exposure to ionizing radiation: gels.** Cultures of hamster CHO cells were exposed to 200 Gy (12 min at 18 Gy/min) at 4–8 °C. The cold medium was replaced by medium at 39 °C (except sample A, which was harvested immediately), and the cultures were allowed to recover for 20 s (B), 1 min (C), 3 min (D), 9 min (E), 15 min (F), 30 min (G), 60 min (H) or 90 min (I). Histones were extracted and analyzed as described under “Experimental Procedures.” TIFF images of the Coomassie Blue-stained gels of histones H2A1 and H2AX were recorded with the Eagle-eye II (Stratagene Cloning Systems). The position of the main novel component is noted as  $\gamma$  with an arrow when it is present and with a dotted line when it is absent or present in a very low amount.

$\gamma$ -components; the same grid is reproduced in Fig. 9B with modification sites, as noted in the H2AX sequence (Fig. 7), assigned to each of the nine forms. The pattern of ubiquitinated forms is identical to that of the nonubiquitinated forms (Fig. 6B, inset), except that each H2AX molecule also contains a ubiquitin modification on residue lysine 119. These assignments also provide an explanation for the different relative amounts of a second faster  $\gamma$ -component seen in mouse and human cells (second arrow in Fig. 2, F–H, and Fig. 3, A and E). Mouse H2AX contains a serine residue at position 136 as well as at position 139 (31), while the human form has a threonine residue at position 136. If serine is the preferred substrate for the kinase, then mouse  $\gamma$ -H2AX might be expected to contain more of a doubly  $\gamma$ -phosphorylated H2AX.

**$\gamma$ -H2AX Forms within Seconds after Exposure of Cells to Ionizing Radiation**—Ionizing radiation can be delivered in precisely measured amounts and time periods. In addition, its effects on cells have been intensively investigated qualitatively and quantitatively; ionizing radiation from  $^{137}\text{Cs}$  results in 35 DNA double-stranded breaks/G<sub>1</sub> genome in mammalian cells (13, 26, 32). These parameters enable us to determine the kinetics and stoichiometry of  $\gamma$ -H2AX formation. To determine how quickly  $\gamma$ -components form after exposure to ionizing ra-

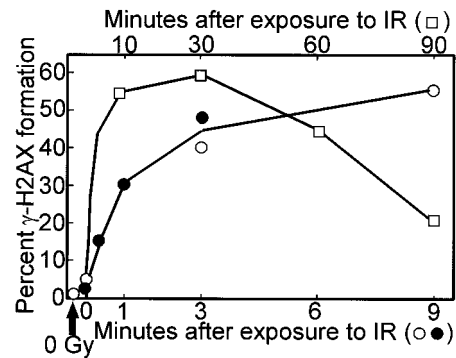


**FIG. 11. Relative amount of  $\gamma$ -H2AX at various times after exposure to ionizing radiation: quantitation.** The H2AX components on the TIFF images presented in the upper panel were quantitated with ImageQuant software version 3.3 (Molecular Dynamics) without any contrast or brightness enhancement. The open circle indicated by the arrow (lower left) shows the percentage of  $\gamma$ -H2AX measured in unirradiated cells. The open and filled symbols denote separate experiments.

diation, hamster CHO cell cultures were irradiated on ice with 200 Gy from a  $^{137}\text{Cs}$  source, rapidly returned to 37 °C, and allowed to recover for various times.  $\gamma$ -H2AX did not form in cell cultures on ice but was visible 20 s after returning them to 37 °C (Fig. 10B).  $\gamma$ -H2AX increased in amount within 10 min to more than 50% of the total H2AX (Fig. 10, C–F), remained at that level until about 30 min postirradiation (Fig. 10G), and then decreased over a period of hours (Fig. 10, H–I). Densitometric analysis of the amounts of H2AX and  $\gamma$ -H2AX from the gels presented in Fig. 10 is shown in Fig. 11. The data form a smooth curve with a rapid rise and a slower decrease. While the maximum is reached at 9–30 min, half the maximum is reached in 1 min. Although these experiments were performed with large amounts of ionizing radiation to obtain a significant signal at short times, similar time courses are observed at lower amounts (data not shown). However, with mice at non-lethal amounts of ionizing radiation, quantitation of the images presented in Fig. 2, E–G, yielded values of approximately 2%  $\gamma$ -H2AX at 15 min (Fig. 2F), 5% at 40 min (Fig. 2G), and less than 2% at 70 min (data not shown), a time course consistent with that shown in Fig. 11. Because of these results, 30 min was chosen as the optimum recovery time when other parameters were studied. Incubation of the irradiated cultures with the protein synthesis inhibitor cycloheximide (100  $\mu\text{g}/\text{ml}$ ) did not prevent  $\gamma$ -phosphorylation (data not shown), indicating that any proteins necessary for  $\gamma$ -modification are already present. Likewise, inhibiting DNA replication with hydroxyurea (10 mM) had no effect on  $\gamma$ -H2AX formation.

**$\gamma$ -H2AX Formation Is Proportional to the Amount of Radiation**—When hamster CHO cell cultures were subjected to different amounts of ionizing radiation, the fraction of  $\gamma$ -H2AX

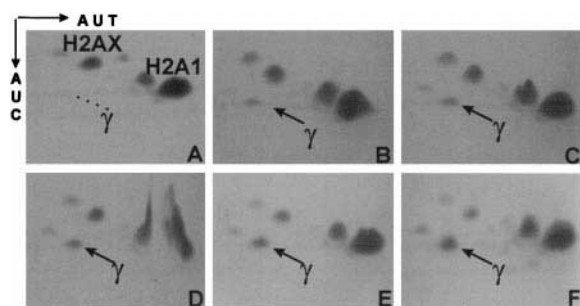


**FIG. 12. The relative amount of  $\gamma$ -H2AX is proportional to the amount of radiation: gels.** Cultures of hamster CHO cells were exposed to 0 (A), 12.5 (B), 25 (C), 50 (D), 100 (E), or 200 (F) Gy of ionizing radiation and permitted to recover at 37 °C for 30 min. Histones were extracted from the cultures and analyzed as described. TIFF images of the Coomassie Blue-stained gels of histones H2A1 and H2AX were recorded with the Eagleeye II (Stratagene Cloning Systems). The position of the main novel component is noted as  $\gamma$  with an arrow when it is present and with a dotted line when it is absent or present in a very low amount.

was found to increase with the amount of radiation (Fig. 12, A–F). Densitometric analysis of the data is presented in Fig. 13. The initial slope of the curve for CHO cells (filled circles) indicates that about 1.0% of the H2AX complement became  $\gamma$ -modified per Gy of radiation. This value may be underestimated because it assumes that all of the relevant H2AX is in the  $\gamma$ -modified state simultaneously. On the other hand, the H2AX in hamster CHO cultures receiving 200 Gy became 67%  $\gamma$ -modified (Fig. 11F) after a 30-min recovery, indicating that the maximal value of  $\gamma$ -H2AX modification is probably no more than 1.5% per Gy for CHO cells. Results with the normal human fibroblast line IMR90 were found to be very similar to those obtained with CHO cells (data not shown).

Densitometric results are also shown for SF268 cultures (Fig. 13, open symbols).  $\gamma$ -H2AX formation in this cell line appears to be more sensitive to ionizing radiation, perhaps related to its high relative content of H2AX. Note that with SF268, the amount of  $\gamma$ -H2AX induced per Gy at the survivable amounts of radiation, 1.2 and 3.6 Gy (Fig. 2, B and C; Fig. 13, arrows) is similar to that induced at the low nonsurvivable amounts, indicating that  $\gamma$ -H2AX formation seen under lethal conditions is the same process as that seen under survivable conditions. The efficiency of  $\gamma$ -H2AX formation is similar in mice. At 40 min postirradiation (Fig. 2G), formation of  $\gamma$ -H2AX was approximately 1.4% per Gy, results comparable with those found in cell culture (Fig. 13).

**$\gamma$ -H2AX Modification and the Relative Abundance of H2AX—**Previous data have shown that the fraction of H2AX converted to  $\gamma$ -H2AX forms is similarly dependent on the amount of ionizing radiation in both CHO cells and normal human IMR90 fibroblasts. Both these cell lines contain H2AX as 9–10% of the total H2A complement. However, we have investigated  $\gamma$ -H2AX formation in cell lines with H2AX comprising as little as 2.4% and as much as 25% of the total H2A complement (Table II). Since the number of DNA double-stranded breaks introduced per Gy per unit of chromatin is the same irrespective of cell lineage (13), this variation enables us to ask whether there is a constant number or a constant percentage of  $\gamma$ -H2AX molecules formed per DNA double-stranded break. The data in Table II are consistent with a similar percentage but not a similar number of H2AX molecules being  $\gamma$ -phosphorylated per DNA double-stranded break; each Gy of ionizing radiation leads to the  $\gamma$ -phosphorylation of about 1–2% of the H2AX irrespective of whether the H2AX accounts for 2.5 or 25% of the total H2A complement. With the variation in its relative abundance, H2AX is unlikely to be localized to certain specific regions of

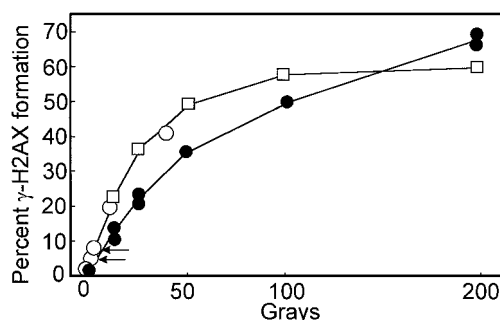


**FIG. 13. The relative amount of  $\gamma$ -H2AX is proportional to the amount of radiation: quantitation.** Filled circles, the H2AX components on the TIFF images presented in the upper panel along with a duplicate set of cultures exposed separately were quantitated with ImageQuant software version 3.3 (Molecular Dynamics) without any contrast or brightness enhancement. Open circles and squares, quantitation of two similar experiments performed with human SF268 cell cultures allowed to recover for 30 min. The arrows denote the data points from the 1.2- and 3.6-Gy samples shown in Fig. 2, B and C.

the chromatin but is likely to be randomly distributed among the nucleosomes. Supporting this assumption is the fact that in lower eucaryotes most or all of the H2A is H2AX (5). If H2AX is randomly distributed throughout the chromatin, then the fraction of  $\gamma$ -H2AX is a measure of the fraction of the chromatin and hence of the DNA that is involved per Gy. Thus, the simplest explanation for these findings is that a similar region of the chromatin is involved per Gy irrespective of the cell line. One Gy of ionizing radiation causes 35 DNA double-stranded breaks/ $G_1$  genome, which is  $6 \times 10^9$  bp of DNA in mammalian cells. If 1% of the chromatin is involved per 35 DNA double-stranded breaks, then 0.03% is involved in each. 0.03% of  $6 \times 10^9$  bp is  $1.8 \times 10^6$  bp. Thus, one of the intriguing implications of these findings is that megabase regions of chromatin appear to be involved in each DNA double-stranded break.

#### DISCUSSION

H2AX becomes phosphorylated on serine 139 rapidly and extensively after exposure of mammalian cell lines and mice to various procedures that lead to the formation of DNA double-stranded breaks.  $\gamma$ -H2AX formation begins within seconds after exposure to ionizing radiation and rapidly passes through a half-maximal value at 1 min to a maximal value at 9–30 min. DNA double-stranded breaks are repaired by various mechanisms in mammalian cells. One pathway involves the DNA-PK complex that is defective in scid mice (33). Evidence for a second DNA double-stranded break repair system has recently been reported (34); this system, which functions during  $G_2$ , appears to be normal in scid cells. H2AX is a substrate for phosphorylation by DNA-PK *in vitro* (35), and we found that purified DNA-PK  $\gamma$ -phosphorylated purified H2AX *in vitro* (data not shown). However, when we examined several of the cell lines that are known to be deficient in DNA-PK, either in the catalytic subunit or in the Ku subunits (36, 37), neither the C.B-17-SCID mouse cell line (33), nor the V3 hamster mutant line (38), nor the ICR-SCID mouse (39) exhibited a noticeable deficit in  $\gamma$ -H2AX formation after exposure to ionizing radiation. With the above mentioned mutant cell lines and mice, it is also possible that residual DNA-PK activity is present, since these are not knockouts. A cell line from the Ku80 knockout mouse (40) was donated by Gloria Li. This line also showed normal  $\gamma$ -H2AX formation. Thus,  $\gamma$ -H2AX formation could result from another DNA double-stranded break repair system that does not utilize DNA-PK<sub>cs</sub> or from a step upstream of DNA-PK<sub>cs</sub> action.

Human cell line M059J, a mutant line lacking DNA-PK protein (41) donated by Joan Turner did show a substantial

TABLE II  
Constant percentages, not numbers, of H2AX molecules are  $\gamma$ -modified per Gy

The stained H2A2, H2A1, and H2AX species on two-dimensional gels were recorded as TIFF images and quantitated with ImageQuant software version 3.3. The  $\gamma$ -H2AX/H2AX ratio was determined 30 min after exposing the cell cultures to 25 Gy. The following conversion factors and assumptions were used. 1) The mammalian G<sub>1</sub> genome contains  $6 \times 10^9$  bp of DNA, hence about  $30 \times 10^6$  nucleosomes (200 bp/nucleosome) and  $60 \times 10^6$  H2A molecules (2 molecules/nucleosome). 2) 25 Gy induces about 875 DNA double-stranded breaks per G<sub>1</sub> genome. 3) H2AX is randomly distributed in the chromatin.

Cell type	H2AX/total H2A	$\gamma$ -H2AX/total H2AX	No. of H2AX/cell	No. of $\gamma$ -H2AX/cell	No. of $\gamma$ -H2AX/dsb	$\gamma$ -H2AX/dsb	bp of DNA/dsb
	%	%				%	
VA13	2.6	28	$1.6 \times 10^6$	$0.45 \times 10^6$	530	0.033	$2.0 \times 10^6$
HeLa	2.4	30	$1.4 \times 10^6$	$0.45 \times 10^6$	490	0.035	$2.1 \times 10^6$
IMR90	9.8	30	$5.9 \times 10^6$	$1.7 \times 10^6$	2100	0.035	$2.1 \times 10^6$
CHO	9.4	34	$5.6 \times 10^6$	$1.9 \times 10^6$	2240	0.040	$2.4 \times 10^6$
SF268	25	50	$15 \times 10^6$	$7.5 \times 10^6$	8800	0.059	$3.5 \times 10^6$

deficiency in  $\gamma$ -H2AX formation. Fifteen min after 200 Gy, the control M059K line converted over 60% of its H2AX to  $\gamma$ -forms, a value similar to that obtained in other mammalian cell lines. In contrast, the mutant M059J line under the same conditions contained no more than 25%  $\gamma$ -H2AX. Human cells contain about 10 times as much DNA-PK activity as do rodent cells, indicating that there may be important differences in these enzyme systems of the two groups.

The locus for the ataxia-telangiectasia defect is 11q23, close to that of the H2AX. However, three ataxia-telangiectasia cell lines from complementation groups A, C, and D were found to contain H2AX and in addition showed no significant deficit in  $\gamma$ -H2AX formation after exposure to ionizing radiation (data not shown). Thus, the ataxia-telangiectasia kinase (42) is not responsible for  $\gamma$ -H2AX formation after irradiation. The defects in other human genetic radiosensitive diseases are located on other chromosomes, suggesting that these diseases are not due to defective H2AX protein (34). H2AX knockout cell lines and mice will help determine the role of  $\gamma$ -H2AX formation in cellular metabolism. We are currently investigating possible relationships between the kinase responsible for  $\gamma$ -H2AX formation and other kinases.

At the time of maximal modification, H2AX on 1–2% of the chromatin is  $\gamma$ -modified. Since each Gy causes 35 DNA double-stranded breaks/ $6 \times 10^9$  bp, this is an amount of chromatin equivalent to  $1.8$ – $3.5 \times 10^6$  bp of DNA/double-stranded break. While this is a strikingly large amount of chromatin, the DNA double-stranded break is a serious lesion that often leads to chromosomal abnormalities; of the 35 DNA double-stranded breaks/genome per Gy, approximately one will result in a visible chromosomal abnormality, and more may be present that are not detectable by cytological analysis (13). Thus biological systems may have evolved very sensitive detection systems for DNA double-stranded breaks;  $\gamma$ -H2AX formation may function in such a system.

There are several types of hypotheses concerning how the  $\gamma$ -H2AX molecules on these large amounts of chromatin might be arranged relative to the DNA double-stranded breaks. In the first type, H2AX molecules on the strands contiguous to the breaks could be  $\gamma$ -phosphorylated starting near the break and progressing away. The  $\gamma$ -H2AX molecules may then provide binding sites for new components involved in recognition or repair or alternatively may lead to conformational changes in the chromatin conducive to DNA repair and cell survival. In the crystallographic structure of the nucleosome (3), H2A lysine 119 is situated at the edge of the nucleosome where the DNA double helices enter and exit. An extended peptide of 20 amino acid residues from lysine 119 to serine 139 has a maximum length of 6 nm, while the nucleosome particle itself has a diameter of 11 nm. Thus H2AX serine 139 has a potential range that covers part of the nucleosome and the histone H1-containing spacer region between nucleosomes. Being on the

exterior of the nucleosome would make H2AX residue serine 139 easily accessible to kinases. If kinases tracked along the DNA about equal distances from a DNA double-stranded break in the various cell lines before falling off or encountering a barrier, then about equal percentages of  $\gamma$ -H2AX would be formed irrespective of relative H2AX content. This model provides an explanation why a constant percentage and not a constant number of the H2AX molecules are  $\gamma$ -phosphorylated per Gy in various cells.

It is not necessary to postulate chromatin structures of megabase dimensions, but there is evidence supporting chromatin structures of this size. Yokota *et al.* (43), measuring the physical distance between probes of known separation along the DNA in interphase nuclei, reported a discontinuity between the physical and genomic distances at about  $2 \times 10^6$  bp, indicating that an underlying chromatin structure of this size may be present. In addition, Yunis (44) using preparations of mid-prophase human chromosomes stained with Giemsa was able to discern about 2000 bands/haploid complement; those values yield an average size of  $1.5 \times 10^6$  bp/band.

In a second type of hypothesis, the DNA double-stranded break would still be the initiating point of the  $\gamma$ -H2AX formation, but the activity would diffuse away from the break in three-dimensional space. Thus, H2AX molecules on strands of chromatin near the DNA double-stranded break would become  $\gamma$ -phosphorylated even if those strands were on different chromosomes. In a third type of hypothesis, H2AX molecules at random throughout the nucleus would become phosphorylated in a manner dependent on the amount of radiation. Determining the spatial relationship between the triggering lesion and the  $\gamma$ -H2AX will be useful in elucidating their functional relationship. Antibodies specific to  $\gamma$ -H2AX will be useful in determining the spatial characteristics of the response.

*Acknowledgments*—We gratefully acknowledge Dr. Kurt Kohn for continuing support. Dr. Joan Turner kindly donated the M059J human mutant cell line, and Dr. Gloria Li kindly donated a Ku80  $-/-$  cell line.

#### REFERENCES

1. Van Holde, K. E. (1989) *Chromatin*, Springer-Verlag New York Inc., New York
2. Pruss, D., Hayes, J. J., and Wolffe, A. P. (1995) *BioEssays* **17**, 161–170
3. Luger, K., Mader, A. W., Richmond, R. K., Sargent, D. F., Richmond, T. J. (1997) *Nature* **389**, 251–260
4. Heintz, N. (1991) *Biochim. Biophys. Acta* **1088**, 327–339
5. Baxevasis, A. D., and Landsman, D. (1996) *Nucleic Acids Res.* **24**, 245–247
6. Thatcher, T. H., and Gorovsky, M. A. (1994) *Nucleic Acids Res.* **22**, 174–179
7. West, M. H. P., and Bonner, W. M. (1980) *Biochemistry* **19**, 3238–3245
8. Brownell, J. E., Zhou, J., Ranalli, T., Kobayashi, R., Edmondson, D. G., Roth, S. Y., and Allis, C. D. (1996) *Cell* **84**, 843–851
9. O'Neill, L. P., and Turner, B. M. (1995) *EMBO J.* **14**, 3946–3957
10. Gurley, L. R., D'Anna, J. A., Barham, S. S., Deaven, L. L., and Tobey, R. A. (1978) *Eur. J. Biochem.* **84**, 1–15
11. Bradbury, E. M., Inglis, R. J., and Matthews, H. R. (1974) *Nature* **247**, 257–261
12. Mannironi, C., Bonner, W. M., and Hatch, C. L. (1989) *Nucleic Acids Res.* **17**, 9113–9126
13. Ward, J. F. (1991) *DNA Damage and Repair in Physical and Chemical Mechanisms in Molecular Radiation Biology* (Glass, W. A., and Varma, M. N., eds) Plenum Publishing Corp., New York

14. Whitlock, J. P., Jr., Galeazzi, D., and Schulman, H. (1983) *J. Biol. Chem.* **258**, 1299–1304
15. Bonner, W. M., West, M. H. P., and Stedman, J. D. (1980) *Eur. J. Biochem.* **109**, 17–23
16. Zweidler, A. (1978) *Methods Cell Biol.* **17**, 223–233
17. Pantazis, P., and Bonner, W. M. (1981) *J. Biol. Chem.* **256**, 4669–4675
18. Goldknopf, I. L., Rosenbaum, F., Steiner, R., Vidali, G., Allfrey, V. G., and Busch, H. (1979) *Biochem. Biophys. Res. Commun.* **90**, 269–277
19. West, M. H. P., and Bonner, W. M. (1981) *Nucleic Acids Res.* **20**, 4671–4680
20. Ueda, T., Toyoshima, Y., Moritani, T., Ri, K., Otsuki, N., Kushihashi, T., Yasuhara, H., and Hishida, T. (1996) *Int. J. Radiat. Biol.* **69**, 199–204
21. Hornsey, S. (1957) in *Advances in Radiobiology* (Hevesy, G. C., Forssberg, A. G., and Abbatt, J. D., eds) p. 248, Charles C. Thomas, Springfield, IL
22. Thomson, J. F. (1962) *Radiation Protection in Animals* Reinhold, New York
23. Casarett, A. P. (1968) *Radiation Biology*, Prentice Hall, Englewood Cliffs, NJ
24. Limoli, C. L., and Ward, J. F. (1993) *Radiation Res.* **134**, 160–169
25. Chabner, B., and Longo, D. L. (1996) *Cancer Chemotherapy and Biotherapy: Principles and Practice*, 2nd Ed., pp. 379–393, Lippincott-Raven Publishers, Philadelphia
26. Friedberg, E. C. (1995) *DNA Repair and Mutagenesis*, pp. 1–58, American Society for Microbiology Press, Washington, D. C.
27. Sestili, P., Cantoni, O., Cattabeni, F., and Murray, D. (1995) *Biochim. Biophys. Acta* **31**, 130–136
28. Simpson, R. T. (1978) *Nucleic Acids Res.* **5**, 1109–1119
29. Whitlock, J. P., Jr., Augustine, R., and Schulman, H. (1980) *Nature* **287**, 74–76
30. Cano, E., Barratt, M. J., Mahadevan, L. C. (1992) *Nature* **360**, 116
31. Nagata, T., Kato, T., Morita, T., Nozaki, M., Kubota, H., Yagi, H., and Matsushiro, A. (1991) *Nucleic Acids Res.* **19**, 2441–2447
32. Ward, J. F. (1994) *Int. J. Radiat. Biol.* **66**, 427–432
33. Kirchgessner, C. U., Patil, C. K., Evans, J. W., Coumo, C. A., Fried, L. M., Carter, T., Oettinger, M. A., and Brown, J. M. (1995) *Science* **267**, 1178–1182
34. Lee, S. E., Mitchell, A., Cheng, A., and Hendrickson, E. A. (1997) *Mol. Cell. Biol.* **17**, 1425–1433
35. Anderson, C. W. (1993) *Trends Biochem. Sci.* **18**, 433–437
36. Thompson, L. H., and Jeggo, P. A. (1996) *Mutat. Res.* **337**, 131–134
37. Zdzienicka, M. Z. (1995) *Mutat. Res.* **336**, 203–213
38. Thompson, L. H., Rubin, J. S., Cleaver, J. E., Whitmore, G. F., and Brookman, K. (1980) *Somatic Cell Genet.* **6**, 391–405
39. Orcutt, R. P., and Gielstfeld, J. G. (1993) *Association for Gnotobiotics, 31st Annual Meeting, Nashville, TN, Nov 14–16, 1993*, (Abstr. 12)
40. Nussenzweig, A., Chen, C., da Costa Soares, V., Sanchez, M., Sokol, K., Nussenzweig, M. C., and Li, G. (1996) *Nature* **382**, 551–555
41. Lees-Miller, S. P., Godbout, R., Chan, D. W., Weinfeld, M., Day, R. S., III, Barron, G. M., and Allalunis-Turner, J. (1995) *Science* **267**, 1183–1185
42. Savitsky, K., Bar-Shira, A., Gilad, S., Rotman, G., Ziv, Y., Vanagaite, L., Tagle, D. A., Smith, S., Uziel, T., Sfez, S., Ashkenazi, M., Pecker, I., Frydman, M., Harnik, R., Patanjali, S., Simmons, A., Clines, G. A., Sartiel, A., Gatti, R. A., Chessa, L., Sanal, O., Lavin, M. F., Jaspers, N. G. J., Taylor, A. M. R., Arlett, M., Collins, F. S., and Shiloh, Y. (1995) *Science* **268**, 1749–1653
43. Yokota, H., van den Engh, G., Hearst, J., Sachs, R., and Trask, B. (1995) *J. Cell Biol.* **130**, 1239–1249
44. Yunis, J. J. (1981) *Human Genet.* **56**, 293–298